Control of Otoacoustic Emission Scattering Waveform with Anti-Noise

Mosheh T. Moskowitz, Montien Saubhayana, Louiza Sellami, and Robert W. Newcomb

Microsystems Lab., Department of Electrical and Computer Engineering University of Maryland, College Park, MD 20742.
e-mails: mosheht@eng.umd.edu, geemsb@eng.umd.edu sellami@eng.umd.edu, newcomb@eng.umd.edu

ABSTRACT

We demonstrate a framework for eliminating significant perturbations along a cascade scattering model of the inner ear. This allows for the conception of a novel scheme of acute anti-noise stimulation at the cochlear level that can be particularly applicable to the class of tinnitus (ringing in the ear) that is aurally originated (peripheral). Peripherally induced tinnitus is often associated with the occurrence of spontaneous and evoked otoacoustic emissions, partially described by Kemp Echos, the basis of the scattering cochlea model ([1]). We propose that a refined version of the work presented here can be fit to individuals with hearing-loss induced tinnitus.

1. Introduction

It is well known that subjecting a patient to either white noise, or noise that is fitted to the approximate frequency region and amplitude of their tinnitus; or to an opposite phase sinusoid of equal tone and amplitude to that perceived, are both cost effective methods of tinnitus reduction. It is estimated that 80% of adults are subject to a form of tinnitus [2], [3], but about a third of those, have it centrally (neurologically) originated, exhibiting asymmetric collicular activity in MRI's that additive noise can not lessen [3]. The technique described below is suitable for those persons expressing tinnitus arising from inner-ear damage (most likely from a noise induced threshold shift) that is measured by a noticeable change of input-output characteristic (or Kemp Echo, see [4]).

The below derivations are built on this input-output characteristic model, which is described in [1], found by fitting parameters to movable fluid mass situated in a cochlear environment. This environment can be described mechanically as shown in Fig. 1a, and more symbolically, as in Fig. 1b. An acoustic waveform exerts pressure on the oval window that in turn, stimulates fluid movement inside the scala vestibuli and media. The basilar membrane divides those scala with that of the tympanic, and has varying stiffness along its length, to resonate with increasing frequency values contained in the input waveform. The cochlea's scattering matrix, θ, initially found from single-input, single-output measurements, is reduced to a number of multiple-input, multiple-output θ's.

When a portion of the basilar membrane vibrates, it elongates a set of inner and outer hair cells within itself to initiate an ionic flow cycle that ultimately propagates neural spike discharges through the auditory nerve (this response is described more thoroughly in pp. 125-138 of [5], but is not included in the analysis of [1], and although is instrumental as to the percept of tinnitus, will be referred to as scattering matrix H as shown in Fig. 2). Signal recognition is often associated with oscillation synchrony, expressed as neural synchrony in so-called live and neural networks, [6], inextricably connected with peripherally-induced tinnitus perception, [7]. One can draw the conclusion from several related publications that noise-induced tinnitus arises from a shifted critical oscillation region, said to be expressed in all wide-dynamic-range sensory systems in [8], and particularly in hearing, as a result of a hysteretic hair cell region, resulting from negative-stiffness induced hair-cell orientations, [9].

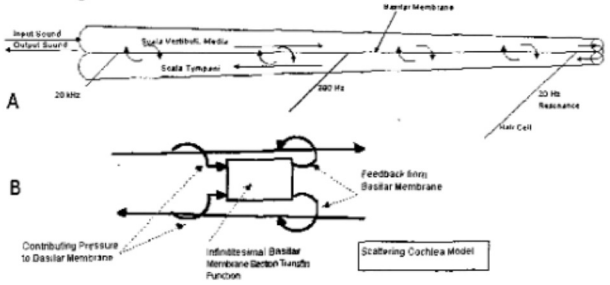

Figure 1 A) Mechanical analogy of the inner ear: the cochlea, and stemming hair cells. B) The analytical analogy of the cochlea to the scattering matrix.

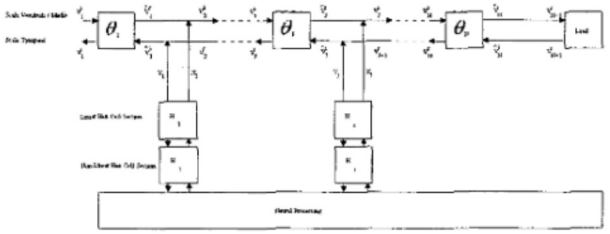

Figure 2 θ represents the cochlear tubules, and H, the hair cells. A defective H is hypothesized to mediate phantom noise, due to a degenerated feedback mechanism in the tuned oscillation region, [8], [9].

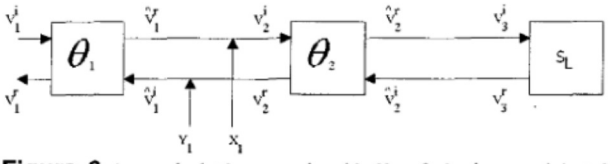

Figure 3 A sample lattice cascade with $N = 2$, having one injected disturbance source, x_1, and y_1 is set to zero.

0-7803-7150-X/01/$10.00@2001 IEEE

2. Formalism

We make use of the abbreviations:

$$\mathbf{V_j} = \begin{bmatrix} v_j^i \\ v_j^r \end{bmatrix} \quad (2.1) \qquad \hat{\mathbf{\Lambda}}_\mathbf{j} = \begin{bmatrix} \hat{v}_j^r \\ \hat{v}_j^i \end{bmatrix} \quad (2.2); \text{ and } \quad \boldsymbol{\xi}_\mathbf{j} = \begin{bmatrix} -x_j \\ y_j \end{bmatrix} \quad (2.3).$$

Here, v_i and v_r are scalar incident and reflected waveforms, and x_j, y_j are scalar noise waveforms arising from hair cell oscillations.

A consecutive series of numbers M through N will be denoted $(.)_{M\subset N}$ or simply $(.)_N$ when $M = 1$. This allows for:

$$\boldsymbol{\theta}_{\mathbf{M}\subset\mathbf{N}} = \prod_{\mathbf{k=M}}^{\mathbf{N}} \theta_k \quad (2.4); \quad \boldsymbol{\Psi}_{\mathbf{M}\subset\mathbf{N}} = \begin{bmatrix} \mathbf{X} \\ \mathbf{Y} \end{bmatrix}_{\mathbf{M}\subset\mathbf{N}} = \sum_{j=M}^{N} \boldsymbol{\theta}_{\mathbf{M}\subset\mathbf{j}} \cdot \boldsymbol{\xi}_\mathbf{j}, \quad (2.5)$$

θ_j, a 2 x 2 scattering matrix:

$$\begin{bmatrix} v_j^i \\ v_j^r \end{bmatrix} = \theta_j \cdot \begin{bmatrix} \hat{v}_j^r \\ \hat{v}_j^i \end{bmatrix} = \begin{bmatrix} \theta_{j_{11}} & \theta_{j_{12}} \\ \theta_{j_{21}} & \theta_{j_{22}} \end{bmatrix} \cdot \begin{bmatrix} \hat{v}_j^r \\ \hat{v}_j^i \end{bmatrix}, \quad (2.6)$$

and:

$$\boldsymbol{\Sigma}_{\mathbf{M}\subset\mathbf{N}} \doteq \frac{\boldsymbol{\theta}_{\mathbf{M}\subset\mathbf{N}11} + \boldsymbol{\theta}_{\mathbf{M}\subset\mathbf{N}12} S_L}{\boldsymbol{\theta}_{\mathbf{M}\subset\mathbf{N}21} + \boldsymbol{\theta}_{\mathbf{M}\subset\mathbf{N}22} S_L}, \quad (2.7)$$

with S_L, a scalar.

3. Finding $v_{j+1}{}^i$ as a function of $v_1{}^i$

Following (2.6):

$$\mathbf{V_j} = \theta_j \hat{\mathbf{\Lambda}}_\mathbf{j}. \quad (3.1)$$

and:

$$\hat{\mathbf{\Lambda}}_\mathbf{j} = \mathbf{V_{j+1}} + \boldsymbol{\xi}_\mathbf{j}. \quad (3.2)$$

It follows from the substitution of (3.1) into (3.2), that:

$$\mathbf{V_j} = \theta_j \mathbf{V_{j+1}} + \theta_j \boldsymbol{\xi}_\mathbf{j}. \quad (3.3)$$

Recursively substituting (3.3) into itself for progressive j, we find that:

$$\mathbf{V_1} = \boldsymbol{\theta}_\mathbf{j} \mathbf{V_{j+1}} + \boldsymbol{\Psi}_\mathbf{j}. \quad (3.4)$$

To calculate a front-end input, $v_1{}^i$, from (3.4) we can use the identity at the terminal section (the section subsequent to the N-th):

$$\begin{bmatrix} v_{N+1}^i \\ v_{N+1}^r \end{bmatrix} = \begin{bmatrix} 1 \\ S_L \end{bmatrix} v_{N+1}^i, \quad (3.5)$$

evident from the right-most section of Fig. 2. Setting $j = N$, in combining (3.4) and (3.5):

$$\mathbf{V_1} = \boldsymbol{\theta}_\mathbf{N} \begin{bmatrix} 1 \\ S_L \end{bmatrix} v_{N+1}^i + \boldsymbol{\Psi}_\mathbf{N}, \quad (3.6)$$

or in matrix fom:

$$\begin{bmatrix} v_1^i \\ v_1^r \end{bmatrix} = \begin{bmatrix} \boldsymbol{\theta}_{\mathbf{N}11} + \boldsymbol{\theta}_{\mathbf{N}12} S_L \\ \boldsymbol{\theta}_{\mathbf{N}21} + \boldsymbol{\theta}_{\mathbf{N}22} S_L \end{bmatrix} v_{N+1}^i + \begin{bmatrix} \mathbf{X} \\ \mathbf{Y} \end{bmatrix}_\mathbf{N}. \quad (3.7)$$

Dividing the expanded top row of (7) by its bottom row:

$$\frac{v_1^i - \mathbf{X_N}}{v_1^r - \mathbf{Y_N}} = \frac{\boldsymbol{\theta}_{\mathbf{N}11} + \boldsymbol{\theta}_{\mathbf{N}12} S_L}{\boldsymbol{\theta}_{\mathbf{N}21} + \boldsymbol{\theta}_{\mathbf{N}22} S_L} \quad (3.8)$$

which is more compactly written with (2.7) as:

$$v_1^r = \frac{v_1^i - \mathbf{X_N}}{\boldsymbol{\Sigma}_\mathbf{N}} + \mathbf{Y_N}, \quad (3.9)$$

or in matrix notation:

$$\begin{bmatrix} v_1^i \\ v_1^r \end{bmatrix} = v_1^i \begin{bmatrix} 1 \\ 1/\boldsymbol{\Sigma}_\mathbf{N} \end{bmatrix} + \begin{bmatrix} 0 \\ \mathbf{Y_N} - \mathbf{X_N}/\boldsymbol{\Sigma}_\mathbf{N} \end{bmatrix}. \quad (3.10)$$

We now solve for an arbitrary section by finding the necessary unknowns of (3.4), i.e., the constituents of $\mathbf{V_{j+1}}$. For compactness, we will have $k = j + 1$:

$$\mathbf{V_k} = \boldsymbol{\theta}_{\mathbf{k}\subset\mathbf{N}} \mathbf{V_{N+1}} + \boldsymbol{\Psi}_{\mathbf{k}\subset\mathbf{N}}, \quad (3.11)$$

and using (3.5), and matrix notation:

$$\begin{bmatrix} v_k^i \\ v_k^r \end{bmatrix} = \begin{bmatrix} \boldsymbol{\theta}_{\mathbf{k}\subset\mathbf{N}11} & \boldsymbol{\theta}_{\mathbf{k}\subset\mathbf{N}12} \\ \boldsymbol{\theta}_{\mathbf{k}\subset\mathbf{N}21} & \boldsymbol{\theta}_{\mathbf{k}\subset\mathbf{N}22} \end{bmatrix} \begin{bmatrix} 1 \\ S_L \end{bmatrix} v_{N+1}^i + \begin{bmatrix} \mathbf{X} \\ \mathbf{Y} \end{bmatrix}_{\mathbf{k}\subset\mathbf{N}}. \quad (3.12)$$

We now readily solve for $v_k{}^i$:

$$v_k^r = \frac{\boldsymbol{\theta}_{\mathbf{k}\subset\mathbf{N}21} + \boldsymbol{\theta}_{\mathbf{k}\subset\mathbf{N}22} S_L}{\boldsymbol{\theta}_{\mathbf{k}\subset\mathbf{N}11} + \boldsymbol{\theta}_{\mathbf{k}\subset\mathbf{N}12} S_L} (v_k^i - \mathbf{X}_{\mathbf{k}\subset\mathbf{N}}) + \mathbf{Y}_{\mathbf{k}\subset\mathbf{N}} \quad (3.13)$$

$$= v_k^i / \boldsymbol{\Sigma}_{\mathbf{k}\subset\mathbf{N}} + \mathbf{Y}_{\mathbf{k}\subset\mathbf{N}} - \mathbf{X}_{\mathbf{k}\subset\mathbf{N}} / \boldsymbol{\Sigma}_{\mathbf{k}\subset\mathbf{N}}$$

which further reduces (3.12) to:

$$\begin{bmatrix} v_k^i \\ v_k^r \end{bmatrix} = \boldsymbol{\theta}_{\mathbf{k}\subset\mathbf{N}} \begin{bmatrix} 1 \\ 1/\boldsymbol{\Sigma}_{\mathbf{k}\subset\mathbf{N}} \end{bmatrix} v_k^i + \begin{bmatrix} 0 \\ \mathbf{Y}_{\mathbf{k}\subset\mathbf{N}} - \mathbf{X}_{\mathbf{k}\subset\mathbf{N}} / \boldsymbol{\Sigma}_{\mathbf{k}\subset\mathbf{N}} \end{bmatrix}. \quad (3.14)$$

Combining (3.4), (3.10), and (3.14):

$$v_1^i \begin{bmatrix} 1 \\ 1/\boldsymbol{\Sigma}_\mathbf{N} \end{bmatrix} = \boldsymbol{\theta}_\mathbf{N} \begin{bmatrix} 1 \\ 1/\boldsymbol{\Sigma}_{\mathbf{k}\subset\mathbf{N}} \end{bmatrix} v_k^i + \boldsymbol{\theta}_\mathbf{j} \begin{bmatrix} 0 \\ \mathbf{Y}_{\mathbf{k}\subset\mathbf{N}} - \mathbf{X}_{\mathbf{k}\subset\mathbf{N}} / \boldsymbol{\Sigma}_{\mathbf{k}\subset\mathbf{N}} \end{bmatrix} - \begin{bmatrix} 0 \\ \mathbf{Y_N} - \mathbf{X_N}/\boldsymbol{\Sigma}_\mathbf{N} \end{bmatrix} + \begin{bmatrix} \mathbf{X} \\ \mathbf{Y} \end{bmatrix}_\mathbf{j}. \quad (3.15)$$

Expanding (3.15) and then subtracting the bottom from top row:

$$v_1^i = v_k^i \frac{\left[(\boldsymbol{\theta}_{\mathbf{N}11} + \boldsymbol{\theta}_{\mathbf{N}12}/\boldsymbol{\Sigma}_{\mathbf{k}\subset\mathbf{N}}) - (\boldsymbol{\theta}_{\mathbf{N}21} + \boldsymbol{\theta}_{\mathbf{N}22}/\boldsymbol{\Sigma}_{\mathbf{k}\subset\mathbf{N}}) \right]}{1 - 1/\boldsymbol{\Sigma}_\mathbf{N}} + \frac{\left[(\boldsymbol{\theta}_{\mathbf{j}12} - \boldsymbol{\theta}_{\mathbf{j}22}) \cdot (\mathbf{Y}_{\mathbf{k}\subset\mathbf{N}} - \mathbf{X}_{\mathbf{k}\subset\mathbf{N}}/\boldsymbol{\Sigma}_{\mathbf{k}\subset\mathbf{N}}) + \mathbf{Y_N} - \mathbf{X_N}/\boldsymbol{\Sigma}_\mathbf{N} + \mathbf{X_j} - \mathbf{Y_j} \right]}{1 - 1/\boldsymbol{\Sigma}_\mathbf{N}}$$

$$= v_k^i \alpha + \beta$$

$$= (\hat{v}_j^r + x_j)\alpha + \beta. \quad (3.16)$$

4. Elimination of x_j with $v_1{}^i$

From Fig. 2, it is apparent that certain criteria are required for a cancellation at $v_{j+1}{}^i$, with retention of values at neighboring ports. We use $(.)^{(n)}$ to denote the n-th solution satisfying the restraints:

{1} The reflection feeding forward from the j-th section must be equivalent to when it is reduced by subtractive noise, x_j, such that when it encounters additive noise, the two eliminate:

$$\hat{v}_j^{r(n)} = \hat{v}_j^r - x_j \quad \text{s.t. } \hat{v}_j^{r(n)} = v_{j+1}^i. \quad (4.1)$$

{2} The signals elsewhere should retain a certain degree of similarity to their respective original values:

$$\mathbf{V_{h+1}}^{(n)} = \mathbf{V_{h+1}}^{(1)}, \quad (4.2)$$

$$\hat{\mathbf{\Lambda}}_{\mathbf{h}}^{(n)} = \hat{\mathbf{\Lambda}}_{\mathbf{h}}^{(1)}, \tag{4.3}$$

$$\hat{v}_j^{i\,(n)} = \hat{v}_j^{i\,(1)}, \tag{4.4}$$

$$v_{j+1}^{r\,(n)} = v_{j+1}^{r\,(1)}, \tag{4.5}$$

where we have used: $h \in \{1,2,...N\} \cap h \notin \{j\}$.

Additionally the first reflection should be that of an ideal cochlea:

$$v_1^{r(n)} = v_1^{r(ideal)}. \tag{4.6}$$

5. Example: Cancellation inbetween two sections, in a two section system.

Let us follow Fig. 3 using a noise waveform:

$$x_1[nT] = \sin(2\pi \cdot f \cdot nT) + \sin(2\pi \cdot 5 \cdot f \cdot nT) + \sin(2\pi \cdot 0.5 \cdot f \cdot nT + \pi/3) + \sin(2\pi \cdot f \cdot nT + \pi/5), \tag{5.1}$$

setting $y_1 = 0$, and using the class of real lattices in [10]:

$$\theta(a,k,z) = \frac{1}{z-a} \cdot \frac{1}{\sqrt{(1-kk^*)(1-kk^*aa^*)}} \cdot \begin{bmatrix} 1-kk^*aa^* & -k(1-aa^*) \\ -k(1-aa^*)z & -(1-kk^*)a^*z + (1-kk^*aa^*) \end{bmatrix} \tag{5.2}$$

$$\theta_n = \theta(a_n, k_n, z),$$

where z is the unit advance ($X_1[z^{-k}] = x_1[(n-k)T]$). Either using (3.16), or more easily, solving Fig. 3 by inspection:

$$v_1^i = v_1^r \mathbf{\Sigma_2} + x_1(\mathbf{\Sigma_2}\theta_{121} - \theta_{111}) - y_1(\mathbf{\Sigma_2}\theta_{122} - \theta_{112}). \tag{5.3}$$

The denominator of $\mathbf{\Sigma_2}$: $(\theta_1\theta_2)_{21} + (\theta_1\theta_2)_{21} S_L$, has at least one root expressing instability (i.e., outside of the unit circle), which if ignored, would yield a result defeating the purpose of the technique. To eliminate this problem, we set the unstable root to zero, and divide the denominator by the sum of unity, and the negative of the unstable root ($1 - r_{unstable}$). The latter step is to account for the gain loss of making the unstable root zero, [11].

For this simulation, we have: $k_1 = 0.2$, $k_2 = 0.3$, $a_1 = -0.5$, $a_2 = -0.9$, $S_L = 0.4$, $f = 0.01$, and $T = 0.001$. Shown in Fig. 5 is the noise source, x_1, and the lesser signal, the effect of the noise on v_2^i with the additive at the input. Figure 5 shows the effective v_2^i without such an additive.

6. Conclusions

We have shown a computational framework for applying anti-noise masking to a damaged portion of the scattering matrix cochlea model. The variable, ξ, allows for the insertion of hair cell non-linearities, arising from a constructed H, computed from the mechanics of hair-cell myosin motors, modeled extensively in [12] and [13], first hypothesized to act as motors in 1980, [14]. We claim our technique is considerably advantageous over prior forms of masking-sensitive tinnitus. As such, we believe it could reach a bank of patients that normal masking would not have, as this model accounts for physical intricacies not present in a pure filter-bank scheme of the inner ear (the most commonly used).

We are most grateful to R. A. Levine, J. R. Melcher, and I. S. Sigalovsky for useful discussion regarding their research on the determination of neurologically originated tinnitus via imaging and the progression of clinical case studies supporting the hypothesis for somatically induced tinnitus.

References

[1] L. Sellami and R. W. Newcomb, "A digital scattering model of the cochlea," *IEEE Transactions on Circuits and Systems-I*, Vol. 44, No. 2, February 1997, pp. 174-180.

[2] M. F. Heller, and M. Bergman, "Tinnitus aurium in normally hearing persons," *Annals of Otology Rhinology and Laryngology*, Vol. 62, 1963, pp. 73-83.

[3] R. A. Levine, "Somatic (craniocervical) tinnitus and the dorsal cochlear nucleus hypothesis," *American Journal of Otolaryngology* (in press).

[4] D. T. Kemp, "Stimulated acoustic emissions from within the human auditory system," *Journal of the Acoustical Society of America*, Vol. 64, No. 5, 1978, pp. 1386-1391.

[5] C. D. Geisler, *From Sound to Synapse: Physiology of the Mammalian Ear*, Oxford University Press, New York, 1998.

[6] J. J. Hopfield, and C. D. Brody, "What is a moment? Transient synchrony as a collective mechanism of spatiotemporal integration," *Proceedings of the National Academy of Sciences of the USA*, Vol. 98, No. 3, 2001, pp. 1282-1287.

[7] J. J. Eggermont and Y. Sininger, "Correlated Neural Activity and Tinnitus," Chapter 4, pp. 21-34, in *Mechanisms of Tinnitus (J. A. Vernon and A. R. Moller editors)*, Simon and Schuster, Needham Heights, 1995.

[8] S. Camalet, T. Duke, F. Julicher, and J. Prost, "Auditory sensitivity provided by self-tuned critical oscillations of hair cells," *Proceedings of the National Academy of Sciences USA*, Vol. 97, No. 7, March 2000, pp. 3183-3188.

[9] P. Martin, A. D. Mehta, and A. J. Hudspeth, "Negative hair-bundle stiffness betrays a mechanism for mechanical amplification by the hair cell," *Proceedings of the National Academy of Sciences USA*, Vol. 97, No. 22, 2000, pp. 12026-12031.

[10] L. Sellami and R. W. Newcomb, "Synthesis of ARMA filters by real lossless digital lattices," *IEEE Transactions on Circuits and Systems-II: Analog and Digital Signal Processing*, Vol. 43, No. 5, May 1996, pp. 379-386.

[11] K. Ogata, *Discrete-time Control Systems, Second Ed.*, Prentice Hall, Englewood Cliffs, 1995.

[12] F. Julicher, A. Ajdari, and J. Prost, "Modeling molecular motors," *Reviews of Modern Physics*, Vol. 69, No. 4, October 1997, pp. 1269-1281.

[13] S. Camalet and F. Julicher, "Generic aspects of axonemal beating," *New Journal of Physics*, Vol. 2, No. 24, 2000, pp. 24.1-24.23.

[14] J. C. Macarney, S. D. Comis, and J. O. Pickles, "Is myosin in the cochlea a basis for active motility?" *Nature (London)*, Vol. 288, December 1980, pp. 491-492.

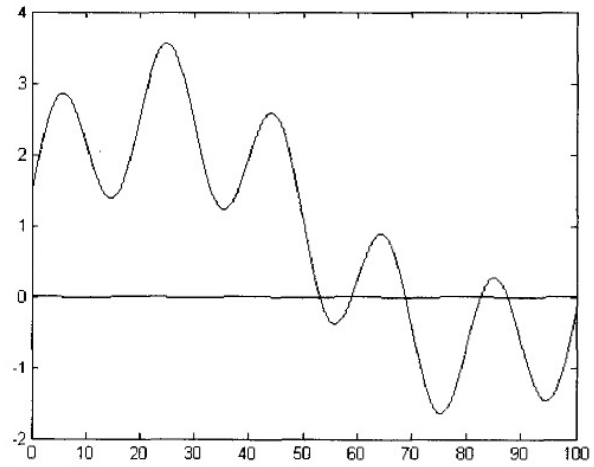

Figure 4 The larger signal is the noise injection (5.1), and the other is the effective v_2^i with an additive signal to v_1^i.

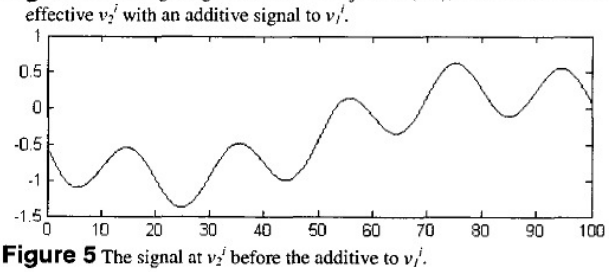

Figure 5 The signal at v_2^i before the additive to v_1^i.